Use of Gated Perfusion To Study Early Effects of Anoxia on Cardiac Energy Metabolism: A New ^{31}P NMR Method†

Randall L. Barbour, Christopher H. Sotak, George C. Levy, and Samuel H. P. Chan*

ABSTRACT: A novel ^{31}P NMR method is described that is capable of determining rapid changes in the intracellular levels of various phosphorus-containing compounds in an isolated, perfused working rat heart. This technique involves the gating of ^{31}P NMR measurements to a heart that is alternately perfused with a modified Krebs–Henseleit medium containing 10 mM pyruvate and equilibrated with either 95% O_2/5% CO_2 or 95% N_2/5% CO_2. The experimental design allows up to three NMR measurements to be made during a single O_2/N_2 perfusion cycle. When these measurements are repeated at different intervals during the cycle, rapid changes in metabolite levels can be determined. Preliminary studies have shown that hearts remain hemodynamically stable to the aerobic/anoxic perfusion cycle as judged by heart rate, peak systolic pressure, aortic output, and coronary flow for at least 80 min in the magnet when subjected to cycle times of 4.5-s O_2 and 1.5-s N_2 perfusions. NMR measurements made under these conditions showed that a transition from full aerobic perfusion to this cycle revealed a new steady state, with an increased inorganic phosphate level from 6% total observable phosphorus to 10% and a possibly significant decreased measurement of creatine phosphate level (from 35 to 31%). Comparison of individual NMR measurements made during this perfusion cycle shows apparent rapid cyclical variations in intracellular pH and the levels of P_i, ATP, and NAD(H). These changes, expressed as variations above and below mean values measured during the cycle, showed that (a) intracellular pH, as measured by the chemical shift of P_i, reversibly decreases by more than 0.1 pH unit within 0.5–1 s following maximal anoxic perfusion and (b) coincident with a decrease in intracellular pH, P_i levels increased by a maximum of 30–40% whereas ATP levels decreased by a maximum of 15–20%. The amount of total observable phosphorus detected during the cycle is essentially constant. Unexpectedly, creatine phosphate levels are most stable, indicating that their levels are being maintained at the expense of ATP. Also unexpected is the finding that NAD(H) levels varied from maximal to undetectable levels during the perfusion cycle. The current method of aerobic/anoxic perfusion is capable of resolving metabolic events much faster than previous NMR methods and yielding information that is unobtainable by any other technique.

Two approaches to examining the effects of anoxia on the levels of high-energy phosphorus metabolites are freeze–clamping followed by enzymatic analysis on neutralized extracts (Williamson & Corkey, 1969) and the more recent use of phosphorus-31 nuclear magnetic resonance spectroscopy. The former technique is easily performed in most laboratories but suffers from being a destructive procedure, thereby obscuring any information concerning possible compartmentation of metabolites. This technique also does not allow examination on the dynamic aspects of metabolism of tissues while maintaining a normal physiological function. In contrast, the use of high-resolution ^{31}P NMR spectroscopy has allowed the dynamic aspects of energy metabolism of tissues to be quantitated nondestructively and repetitively in the intact organ while normal physiological function is preserved. The need for signal averaging, however, largely limits its ability to measure rapid changes in metabolite levels requiring a minimum time of measurement of 30 s for qualitative information and 2–3 min for quantitative information. Despite this limitation, two methods, namely, NMR gating and spin transfer, have been developed that are capable of studying energy metabolism on a much faster time scale. The rationale of gating methods is that, when NMR measurements are timed to the periodic application of stimulus or agent, it is possible to follow changes in the levels of various metabolites during this cycle. For example, Fossel et al. (1980) have shown that, when ^{31}P NMR measurements are gated to the cardiac cycle, variations in the levels of high-energy phosphates could be measured having a potential time-resolution of 2 ms.

Using the freeze–clamp technique, Hearse (1979) reported that, within 2 s following anoxic perfusion, cellular ATP and creatine phosphate levels declined by 15 and 40%, respectively, prior to decline in contractile force. This finding is in apparent contradiction with more recent NMR studies (Hollis et al., 1978; Bailey & Seymour, 1981; Gadian et al., 1981; Flaherty et al., 1982) which have shown that, upon anoxic perfusion, the ATP level remains stable while the creatine phosphate level declines rapidly. Hearse (1979) also reported that the decline in ATP and creatine phosphate levels was biphasic, which reached minimum levels 10–12 s into anoxic perfusion followed by a partial recovery and then a further decline. Whether this reflects an in situ event is not known due to the destructive nature of the freeze–clamp technique and the relative instability of the compounds in strongly acidic conditions. In the present study, we have reexamined the effects of anoxia on the levels of high-energy phosphate compounds by gating NMR measurements to an alternating aerobic and anoxic perfusion cycle. Using this method, we are able to resolve metabolic events (changes in intracellular pH, levels of ATP, creatine phosphate, and P_i) much faster than previous NMR studies.

Materials and Methods

NMR measurements were performed on isolated rat hearts that were perfused in either the Langendorff (Langendorff,

† From the Department of Pathology, SUNY Downstate Medical Center (R.L.B.), and the Departments of Chemistry and Biology, Syracuse University, Syracuse, New York 13210 (C.H.S., G.C.L., and S.H.P.C.). *Received January 17, 1984.* This work was supported by the NIH Biotechnology Research Resource for Multi-Nuclei and Data Processing (NIH Grant RR-01317 and NIH Grants RR-05401 and CA-20454). Parts of this work were presented at the 1983 meeting of the American Society of Biological Chemists, San Francisco, CA (Barbour et al., 1983).

* Address correspondence to this author at the Department of Biology, Syracuse University.

0006-2960/84/0423-6053$01.50/0

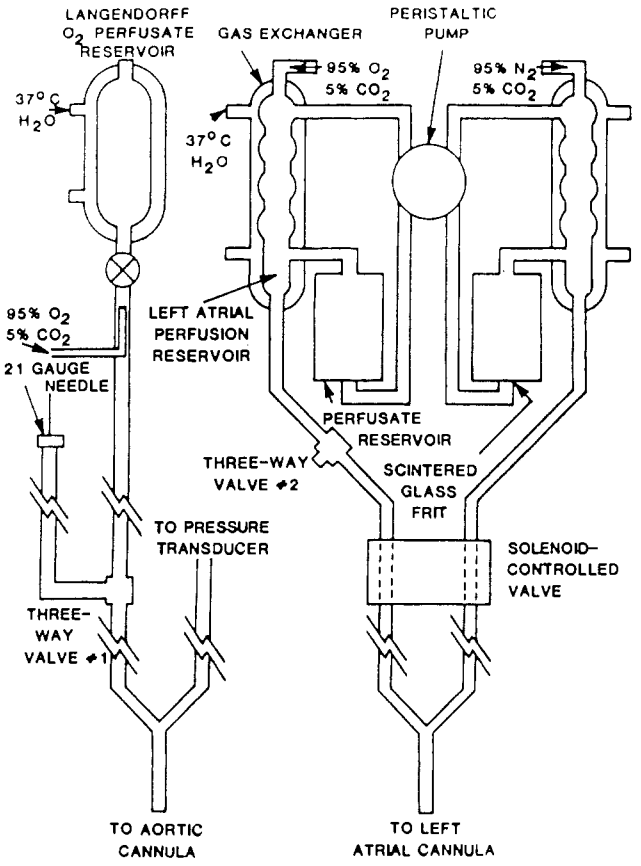

FIGURE 1: Schematic of the alternating perfusion apparatus.

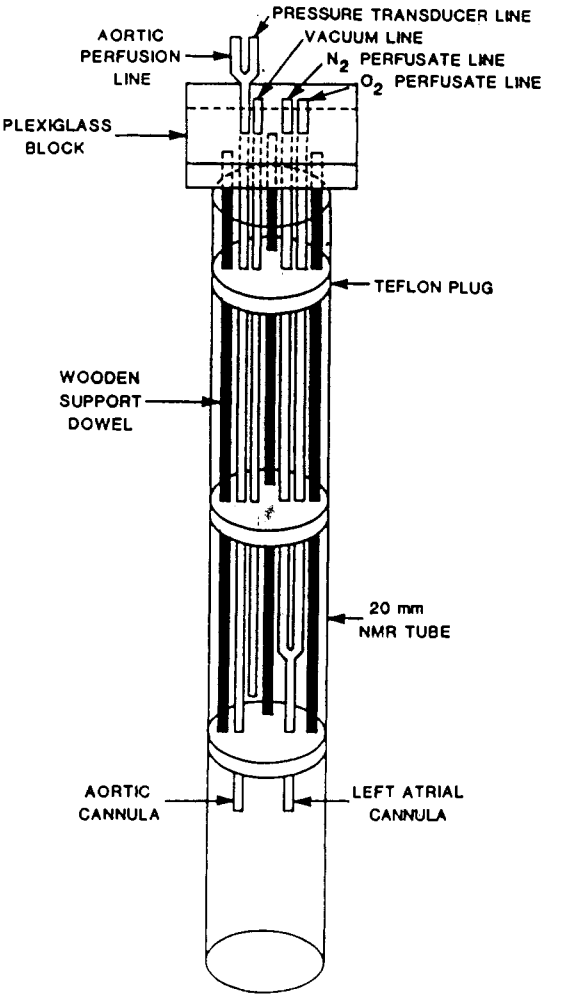

FIGURE 2: Schematic of the cannula assembly employed in the NMR probe for the perfused heart experiment.

1895; Morgan et al., 1961) or working (Neeley et al., 1967) modes. Both these preparations have been described in detail (Neeley & Rovetto, 1975).

Aerobic/Anoxic Perfusion Apparatus. The apparatus used in the perfusion cycle experiments consists of a Langendorff perfusion apparatus in conjunction with two working heart perfusion apparatuses functioning in parallel: one containing perfusate gassed with 95% O_2/5% CO_2 and the other gassed with 95% N_2/5% CO_2. This is illustrated schematically in Figure 1. The solenoid-controlled valve was fabricated in-house and simultaneously opens one of the perfusion lines while closing the other.

The oxygen perfusion line contains a three-way valve (no. 2 in Figure 1) between the solenoid-controlled valve and the left atrial perfusion reservoir. This valve is closed during nonworking mode portions of the experiment since the default state of the solenoid-controlled valve constricts only the nitrogen perfusion line, leaving the oxygen perfusion line open.

Cannula Assembly. The cannula assembly for perfusing the heart is shown in Figure 2. This structure supports three perfusion lines, a vacuum line to remove coronary effluent, and a pressure transducer line that intersects the aortic perfusion line via a Y-tube just above the plexiglass block. The working mode oxygen and nitrogen perfusion lines intersect at a Y-tube positioned just above the left atrial cannula. The assembly is designed to fit within a 20-mm NMR tube, and the two cannulas are positioned such that the heart can contract freely without touching the sides of the NMR tube. The vacuum line for removing coronary effluent is positioned just above the lower Teflon plug.

The tubing connecting the cannula assembly and perfusion reservoirs comprise an approximately 10-ft "umbilical" that allows the cannula assembly to be inserted into the NMR magnet while the perfusion apparatus itself remains a safe distance from the magnet field. As much of the umbilical as possible is water jacketed to ensure that the temperature of the perfusate remains constant. The umbilical water jacket and those of all perfusion reservoirs are maintained at 37 °C with a circulating heating bath.

Hardware Interface between Spectrometer Computer and Perfusion Apparatus. The hardware interface between the spectrometer computer and the solenoid-controlled valve of the perfusion apparatus consists of a lever assembly that simultaneously constricts one of the perfusion lines, by compressing the tubing, while permitting unrestricted flow in the other. The lever assembly is attached by two flexible plastic cables to two pull-type AC heavy-duty solenoids. Constriction of a particular perfusion line is implemented by supplying power to the appropriate solenoid. A 12-V relay is actuated by an in-house designed timer circuit. The duration of anoxic perfusion is switch selectable in a range from 1 ms to 10 s with 1-ms resolution. The timer circuit is connected by coaxial cable to the decoupler transmitter channel output on the back of the spectrometer computer. Anoxic perfusion is initiated by the spectrometer computer with a 1-ms TTL (transistor transistor logic) pulse on the decoupler transmitter channel that is under software control.

Perfusion Medium. The perfusion medium consisted of a modified Krebs–Henseleit (1932) buffer containing components having the following concentrations: 118 mM NaCl, 4.7 mM KCl, 2.5 mM $CaCl_2$, 1.2 mM $MgSO_4$, 1.2 mM

KH_2PO_4, 24 mM $NaHCO_3$, and 10 mM metabolic substrate (either pyruvate or glucose). Preliminary studies showed that hearts were more stable to the alternating perfusion cycle if phosphate was included in the perfusate. The pH of the solution was adjust to 7.4 by gassing with 95% O_2/5% CO_2 or 95% N_2/5% CO_2. Steady-state O_2 levels for these solutions were 600–650 and 35–40 torr, respectively.

Preparation of Rat Hearts. Male Sprague-Dawley rats weighing between 250 and 400 g were anesthetized with ether and injected intraperitoneally with heparin (1500 units/kg) 15 min before use. The heart with the attached lungs was then quickly immersed in a slush of perfusion medium (prepared by addition of dry ice) to induce cardiac arrest. This typically occurred within several seconds.

Cannulation of the Heart. (1) Langendorff Mode. Prior to cannulation, the heart was trimmed of excess thymus, lung, and filamentous tissue. The heart remained in the cold perfusate as much as possible during this procedure. Particular care was taken when the lungs were removed to cut through the point at which the pulmonary veins join the left atrium. The aorta was secured to the cannula by using fine surgical thread. Care was taken not to occlude the pulmonary artery during this procedure. Retrograde perfusion of the coronary vessels was immediately initiated by opening the three-way valve (no. 1 in Figure 1) in the aortic perfusion line. Hearts typically resumed contraction spontaneously within 30 s of perfusion. Perfusion pressure was usually 110 cm of water.

(2) Working Mode. After the heart had been stabilized in the Langendorff mode, the left atrium was cannulated via one of the four pulmonary veins and secured with surgical thread. Proper cannulation of the left atrium was verified by briefly perfusing the heart in the working mode. This involves opening the three-way valve (no. 2 in Figure 1) in the left atrial oxygen perfusion line while simultaneously switching the three-way valve (no. 1 in Figure 1) in the aortic perfusion line from the perfusion reservoir to the perfusate-filled line terminated with the 21-gauge needle. Pressure development and heart rate were measured on a Statham Model P23 Db pressure transducer connected to the aortic line and recorded on the Mennen Greatbatch physiological recorder.

Positioning of the Heart in the NMR Magnet. After satisfactory performance of the heart in the working mode had been verified, the heart was returned to the Langendorff mode in preparation for placing it in the NMR magnet. A capillary tube containing 4% H_3PO_4, to serve as an analytical internal standard, was positioned next to the heart. The cannula assembly with the attached heart was placed inside a 20-mm NMR tube. Coronary effluent was removed from the tube by using a vacuum pump connected to the vacuum line in the cannula assembly. A 1-L Erlenmeyer filtering flask was used as a trap to collect the coronary effluent. This flask was placed on a balance so that the weight, and hence the volume, of coronary flow could be continuously monitored.

The position of the cannula assembly inside the NMR tube was carefully adjusted so that the height of the heart would exactly coincide with the center of the receiver coil when the tube was placed inside the magnet. The top of the tube was secured to the wooden dowel rods of the cannula assembly by using masking tape.

Once the heart was positioned in the magnet, the observe coil of the probe was tuned to 145.8 MHz by using a hybrid junction (Anzac). This procedure was repeated each time a heart was placed in the magnet. Lack of deuterium in the sample precluded the use of field-frequency lock. Sample homogeneity was optimized by monitoring the ^{1}H signal on the observe channel and maximizing the free-induction decay signal from the aqueous buffer (Ackerman et al., 1981).

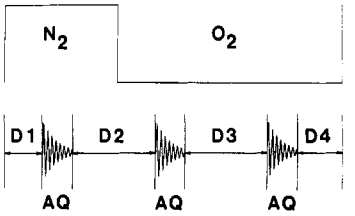

FIGURE 3: Generalized data acquisition timing scheme for an isolated working rat heart alternately perfused under anoxic and aerobic conditions.

NMR Measurements. (1) Instrumentation. The NMR measurements for the perfused rat heart experiments were performed on a Bruker WM-360 wide-bore (73 mm free access) high-resolution NMR spectrometer. This instrument is equipped with a superconducting magnet operating at a magnetic field strength of 8.5 T which corresponds to a ^{31}P resonance frequency of 145.8 MHz. All measurements were performed by using a 20-mm broad-band probe fabricated by Cryomagnet Systems. Data were acquired with a dedicated Aspect 2000 minicomputer running the FTQNMR data acquisition and processing software package. Signal-averaged free-induction decays (FID's) were transferred to a Data General MV-8000 computer where they were processed by using the NMR1 (Dumoulin & Levy, 1981) spectral data analysis system.

(2) Partitioning of Computer Memory for Data Acquisition. The use of the FTQNMR data acquisition and processing software package allows the spectrometer's computer memory to be partitioned into three independent memory areas: one memory block for each "job". Memory is partitioned by entering an integer value for the starting address for the current job memory block. Transfer of program execution from one job block to another occurs almost instantaneously by specifying the desired destination block, J1, J2, or J3, in the Bruker microprogram software utility. This mechanism obviates the need for disk I/O between data acquisitions which usually requires more time than is allowed by the constraints of the experiment.

(3) Data Acquisition Parameters. The cardiac phosphorus-containing metabolites of interest were observed within a spectral width of 5000 Hz corresponding to a chemical shift range of 34.3 ppm. Each FID consisted of 4096 data points (2048 complex data points). The acquisition time was 0.4096 s, and the data were acquired by using a phase alternation scheme. Spectra having acceptable signal-to-noise ratio (S/N) were usually obtained by summing 300 FID's. Excitation pulses were spaced 1.5 or 2.0 s apart, depending upon the duration of the nitrogen/oxygen perfusion cycle and the number of FID's acquired within the cycle. The observed pulse width for a 90° tip angle was typically 40 μs (with 0 dB of pulse power attenuation) and was measured prior to each session. Broad-band decoupling of protons was not employed to avoid complications in the peak area measurements due to differences in nuclear Overhauser enhancement for different resonances. The decoupler control circuitry was modified to trigger the solenoid-controlled valve and allow decoupling, if desired.

(4) Data Acquisition Microprogram and Timing Sequence. Synchronization of data acquisition and perfusate gating is provided by the microprogram software utility in the FTQNMR data acquisition and processing software package. The timing sequence for a typical alternating perfusion experiment is shown in Figure 3, and the following is the corresponding

microprogram to implement this sequence:

1, J1	10, D0	19, D4
2, ZE	11, D1	20, L0 TO 7, TIMES: 300
3, J2	12, G0=12	21, J1
4, ZE	13, J2	22, WR FILENAME #1
5, J3	14, D2	23, J2
6, ZE	15, G0=15	24, WR FILENAME #2
7, J1	16, J3	25, J3
8, BB	17, D3	26, WR FILENAME #3
9, D5	18, G0=18	27, EXIT

Prior to writing the microprogram, the memory is partitioned, and the requisite data acquisition parameters are read into memory in each job block. The commands J1, J2, and J3 transfer program execution to those respective job blocks. The command ZE zeros memory. Steps 1–6 zeros memory in each job block in preparation for data acquisition. Program execution is then returned to job 1 (step 7), and a period of anoxic perfusion is initiated by turning the decoupler control circuitry (BB in step 8) for duration D5 (1 ms) and then turning it off (D0). After preset delay D1, the computer acquires the first FID (step 12). Program execution is transferred to job 2, the computer waits for period D2 and then acquires the second FID (step 15). The last FID is acquired (step 18) after delay D3. The entire cycle is initiated again following waiting period D4, by looping (in step 20) back to step 7, and is repeated as necessary (in this case 300 times) to achieve the desired S/N in the transformed spectrum. Following the acquisition of the desired number of scans in each memory area, program execution is transferred back to job 1 and the contents in memory are written to disk under the specified filename (step 22). This is repeated for the remaining two independent memory areas, and the microprogram terminates with the EXIT statement in step 27.

The position of data acquisitions can be placed almost anywhere within the anoxic–aerobic cycle by varying the delays D1 and D4. Data acquisitions cannot occur during the time that the computer triggers the timer circuit to initiate anoxic perfusion; they must occur just prior to immediately following. This results in three "blind spots" in the cycle, the length of which are determined by the data acquisition time. The delays were chosen such that D2 = D3 = D1 + D4 to avoid differences in spectral resonance intensity as a result of spin saturation effects.

Data Processing. Following transfer to the MV-8000, the signal-averaged FID's were zero filled to 8K and Fourier transformed with 25-Hz line broadening. The resulting spectrum was carefully phased, and spectral base-line artifacts were removed by using an iterative base-line flattening algorithm. Resonances were identified, and their chemical shifts were calibrated to phosphocreatine as 0 ppm. Peak areas were calculated by using a floating point Simpson's rule algorithm with the limits of integration chose as five line widths. Partially resolved peaks were integrated, as necessary, by using the curve-fitting module of NMR1.

Results

Phosphorus-31 spectra obtained from fully oxygenated working mode hearts (Figure 4) show different steady-state levels of phosphorus-containing metabolites when two different metabolic substrates (namely, glucose vs. pyruvate) are used. It should be noted that intracellular inorganic phosphate [P_i(INT)] for healthy pyruvate perfused hearts is almost nonexistent and thus difficult to measure while the phosphocreatine (PCr) level increased up to 35% compared with glucose-perfused hearts. In contrast, signals representing γ-ATP, α-ATP and NAD(H), and β-ATP remain fairly

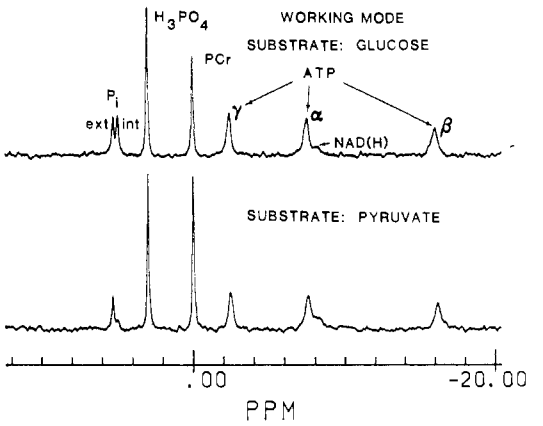

FIGURE 4: Phosphorus-31 NMR spectra of an isolated working rat perfused with glucose (upper trace) and pyruvate (lower trace) as metabolic substrate. Both spectra were acquired from the same heart; the glucose perfused spectrum first, followed by the pyruvate perfused spectrum. The H_3PO_4 signal is an internal standard of 4% phosphoric acid.

constant. These results of different steady-state levels of phosphorus-containing metabolites when perfused with different substrates reinforce our interpretation on observations obtained during alternating perfusion experiments presented below.

Effects of Aerobic/Anoxic Perfusion Cycle on Cardiac Function. Our initial experiments focused on optimizing the conditions in which maximal changes in the levels of phosphorus metabolites were observed during the perfusion cycle while maintaining a functionally stable heart. Cardiac stability was assessed by measuring aortic pressure, heart rate, coronary flow, and aortic output as described under Materials and Methods. Preliminary estimates for the appropriate timing of this cycle were based on the previous study by Hearse (1979), who reported that contractile failure, and the accompanying decline in intracellular energy levels, occurs within 5 s following a transition of aerobic to anoxic perfusion in a working rat heart. Because the current technique requires that the heart remains hemodynamically stable to aerobic/anoxic cycling, we initially concluded that maximal durations or anoxic perfusion must be considerably less than 5 s.

Preliminary studies involving hearts exposed to cycle times 2.5-s O_2/0.5-s N_2 perfusion remained stable for up to 2 h when either 10 mM glucose or 10 mM pyruvate was used as a substrate. The duration of the nitrogen perfusion was subsequently increased and the stability of the hearts measured. Results from these studies indicate that optimal cycle times for hearts perfused with pyruvate are between 4.5 s of O_2/1.5 s of N_2 and 4.0 s/2.0-s of N_2. Under these conditions a transition from full aerobic perfusion to O_2/N_2 cycle reversibly decreases peak systolic pressure, coronary flow, and aortic output by 10–15%; heart rates were unaffected. Hearts remained stable to this cycle for up to 80 min in the magnet as evidenced by less than a 10% decline in pressure development from initial values following a return to full aerobic perfusion. Control values for hearts perfused with pyruvate under full aerobic conditions were the following: heart rate, 240 beats/min; coronary flow 10–12 mL min^{-1} g^{-1} wet weight; aortic output, 4–6 mL min^{-1} g^{-1} wet weight; systolic pressure, 170–210 mmHg at a left atrial filling pressure of 13 cm of H_2O. The relatively high coronary flow and low aortic output stems from positioning the aortic outflow line 60 cm above the heart. Hearts perfused in this fashion exhibited greater stability to the cycle as opposed to having a lower coronary flow and higher aortic output.

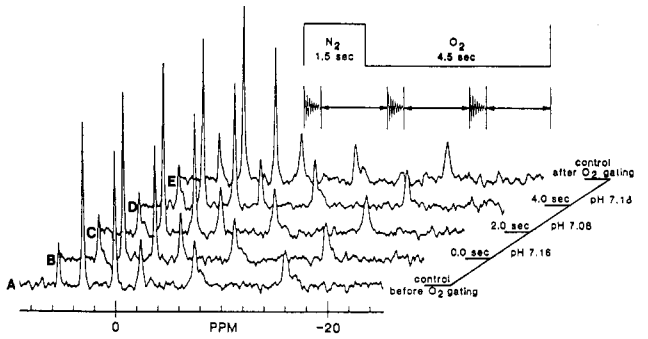

FIGURE 5: Phosphorus-31 NMR spectra of a pyruvate-perfused working rat heart obtained before, during, and after oxygen/nitrogen cycle. The N_2/O_2 perfusate ratio is 1.5/4.5, and the cycle time is 6.0 s. See Figure 4 for identification of the signals.

Table I: Phosphorus-31 Metabolite Levels in Pyruvate-Perfused Working Rat Hearts as a Percentage of Total Phosphate Measured before, during, and after O_2/N_2 Perfusion Cycle

	^{31}P metabolite levels as a percentage of total phosphate				
conditions	P_i	PCr	γ-ATP	α-ATP and NAD(H)	β-ATP
prior to O_2/N_2 cycle ($N = 7$)[b]	6 (3)[a]	35 (2)	19 (1)	20 (3)	20 (3)
during O_2/N_2 cycle ($N = 21$)[b]	10 (3)[c]	31 (2)[d]	19 (2)	21 (3)	19 (2)
after O_2/N_2 cycle ($N = 7$)[b]	10 (3)[c]	33 (1)[e]	19 (3)	21 (4)	17 (2)

[a] Values in parentheses denote ±standard deviation. [b] Number of values used to calculate mean and standard deviation. [c] Significantly increased compared to "prior O_2/N_2 cycle" ($P < 0.002$). [d] Significantly decreased compared to "prior O_2/N_2 cycle" ($P < 0.05$). [e] Significantly increased compared to "during O_2/N_2 cycle" ($P < 0.05$).

Interestingly, under nearly all conditions studied, hearts perfused with pyruvate consistently exhibited greater performance (i.e., higher flow rates and pressure development) than hearts perfused with glucose. Under conditions of full aerobic perfusion pyruvate-perfused hearts exhibited increased values for coronary flow, aortic output, and peak systolic pressure by approximately 25, 25, and 30%, respectively, compared to hearts perfused with glucose. NMR measurements performed on the same heart which was initially perfused with glucose and later with pyruvate showed that this higher level of performance was associated with an approximate 25% increase in steady-state levels of creatine phosphate with a concomitant (and quantitative) decrease in intracellular inorganic phosphate (see Figure 4). This represents a new finding and one that deserves further study. Because it was advantageous to perfuse hearts under conditions having maximal flow rates (see Discussion) all subsequent studies were performed with hearts perfused with 10 mM pyruvate.

Effects of Oxygen/Nitrogen Cycle on Cardiac Energy Metabolism. Spectra shown in Figure 5 and data shown in Table I illustrate the effect that alternating O_2/N_2 perfusion (4.5 s of O_2/1.5 s of N_2) has on steady-state metabolite levels in hearts perfused with pyruvate. Values indicated represent the percentage of the observable phosphorus that a given resonance constitutes as measured by integration after correcting for the presence of orthophosphate in the perfusion medium. This correction was made by measuring the resonance intensity of P_i in the perfusion buffer and, after correcting for the displacement of fluid by the heart, subtracting this value from the integrated area of P_i and total phosphorus in the original spectrum. Typically this value averaged 8% of the total phosphorus measured in an uncorrected spectrum. Inspection of Table I shows that prior to the O_2/N_2 cycle, under conditions of full aerobic perfusion, steady-state P_i levels are low, being only 6% of total, whereas creatine phosphate levels are nearly 6-fold higher (35%). The resonances corresponding to the three phosphates of ATP each average close to 20% of the total. This low level of P_i in well-functioning hearts is in agreement with previous studies (Jacobus et al., 1982).

Values shown during the cycle represent the mean levels from the three spectra obtained at various intervals during the perfusion cycle for each of seven hearts. Because, as shown below, these values are actually undergoing cyclical variations during the cycle, the average shown represents a pseudo-steady-state level. Comparison of these values to values obtained during full aerobic perfusion before and after the O_2/N_2 cycle illustrates, in part, the overall impact that the perfusion cycle has on cellular energy levels.

A transition from full aerobic perfusion to O_2/N_2 cycle results in a significant increase in intracellular P_i levels from 6 to 10% of total and a significant decrease in creatine phosphate levels (from 35 to 31% of total); ATP levels were essentially unaffected. Following a transition back to full aerobic perfusion, P_i levels remain elevated whereas creatine phosphate levels undergo a partial, but significant, recovery. ATP levels again remain unaffect.

The results shown in Table I agree well with the hemodynamic studies showing that, as expected, the overall effect of the O_2/N_2 cycle is to induce a partially hypoxic state. In addition, although statistically significant changes in P_i and creatine phosphate levels were detected as a result of the O_2/N_2 perfusion cycle, these changes were small, indicating that minimal damage to the heart occurs.

As described under Materials and Methods, NMR measurements made during O_2/N_2 cycle are achieved by synchronizing the collection of FID's with the alternate perfusion of the heart by using an in-house designed, solenoid-controlled valve under computer control. Typical changes seen in the resulting NMR spectra compared to spectra obtained before and after O_2/N_2 cycle are shown in Figure 5. In this experiment, hearts were subjected to cycle times of 4.5-s O_2/1.5-s N_2 perfusion, and FID's were collected every 2.0 s. Several important findings are illustrated in this figure. First, comparison of spectra C and B clearly shows the appearance and loss of a second P_i peak corresponding to pH 7.1, demonstrating that changes of 0.1 pH unit occur within 2.0 s during the cycle. Integration of these peaks shows that P_i levels actually increase (by as much as 5% of total observable phosphorus), suggesting that hydrolysis of high-energy phosphates are occurring simultaneously to the production of intracellular acid. The source of this acid remains unidentified, but the formation of lactic acid from pyruvate is strongly suspected. Second, NAD(H) levels are observed to vary from maximal to undetectable levels during the cycle. The low signal to noise associated with this peak prevents accurate quantitation; nevertheless, it is clear that large variations do occur. This observation may indicate that cyclical binding of the coenzymes to proteins occurs during the cycle, resulting in a large increase in its T_1 value. This finding is consistent with a previous report by Chance & Baltscheffsky (1958), who showed that the fluorescence intensity of reduced pyridine nucleotides increases during a state 3 to state 4 transition. Third, the integrated area and line width of the β-ATP resonance are routinely observed to vary during the cycle up to 15–25% and 30–40%, respectively. The former strongly suggests that ATP hydrolysis is occurring whereas variations

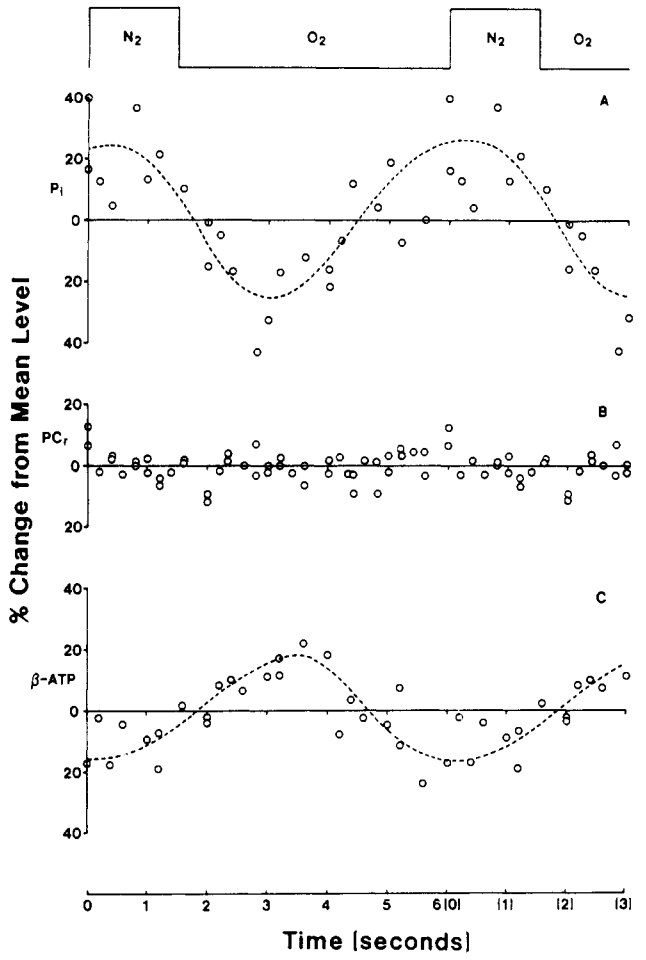

FIGURE 6: Plot of percentage change of intracellular inorganic phosphate (A), phosphocreatine (B), and β-ATP (C) from their respective mean levels within the anoxic–aerobic cycle.

in spectral line widths may stem from exchange broadening due to changes in the proportion of Mg^{2+}-bound ATP (Gadian, 1982).

Most unexpected was the finding that creatine phosphate levels are stable during the O_2/N_2 cycle. We believed that this observation does not necessarily contradict previous reports demonstrating that creatine phosphate levels decline upon the onset of anoxia (Bailey et al., 1981; Matthews et al., 1981a) while ATP levels remain constant. It is important to realize that when the technique of perfusion cycling is used, it is possible to detect changes in metabolite levels much faster than previous NMR studies have achieved. It should be noted that we have varied the duration of the O_2/N_2 cycle from 5 s of O_2/1 s of N_2 to 2 s of O_2/1 s of N_2 and five other cycle times in between. In every case, essentially similar results were observed. Furthermore, when control experiments of alternating the perfusions with both aerobic media were performed, no metabolic oscillations were observed. Thus, it is clear that the metabolic oscillations observed during the O_2/N_2 cycle were real and could not be coincidental with metabolic fluctuations not related to anaerobic perturbations.

Data in Figure 6 summarize the results of nine experiments in which hearts were subjected to perfusion cycles of 4.5 s of O_2/1.5 s of N_2 and NMR measurements were made at various intervals during the cycle. Ordinate values indicate the percent change that individual data points varied from mean values determined from each set of three measurements acquired during the cycle. The precision of measurement based on comparison to an internal standard of phosphoric acid is approximately ±5%, and thus deviations from mean levels by a greater amount represent real changes in metabolite levels. The time zero on the abscissa indicates the time at which the TTL pulse is initiated to open the nitrogen line. It should be noted that approximately up to 1.0 s is required after the pulse to overcome the mechanical inertia in the system and allow flow of the new solution to begin. In addition, on the basis of the dead volume in the cannula assembly and coronary flow rates, approximately up to 3.0 s is required before the "new" solution begins to perfuse the coronary bed. As described under Materials and Methods, the two solutions are joined by a Y connector just prior to entering the left atrium, and thus the transition between aerobic and anoxic perfusion will not be abrupt but rather sinusoidal. Thus, maximal anoxic perfusion would not be expected to occur until about 4.5 s following the TTL pulse to open the nitrogen line. This time represents a minimal value since probably additional time is also required for complete perfusion of the coronary bed to occur and for oxygen to diffuse from the coronary bed to the mitochondrial membrane.

For illustrative purposes data points corresponding to the first 3 s of the cycle are plotted repetitively to indicate the cyclical nature of the changes. The dynamic cyclical changes in the level of the phosphorus metabolites which occur during O_2/N_2 cycle are clearly illustrated in this figure. Results in panel A show that P_i levels vary by 30–40% from mean values during the cycle and that upon anoxic perfusion P_i levels increase. Associated with this increase and decrease in P_i levels is the appearance and disappearance, respectively, of a second P_i peak corresponding approximately to pH 7.1, demonstrating that intracellular pH decreases upon the onset of anoxia. Possible sources accounting for variations in P_i levels are that creatine phosphate and/or ATP hydrolysis occurs during the cycle. Other less likely explanations are that the T_1 value for P_i increases during the cycle and/or that there is a difference in P_i transport across the cell membrane.

Results in panel B demonstrate that creatine phosphate levels remain essentially constant during O_2/N_2 perfusion. This finding is most surprising in view of previous studies which have established that creatine phosphate levels decline upon the onset of anoxia (Hearse, 1979) or ischemia (Bailey et al., 1981; Hollis et al., 1978). We believe, however, this observation does not necessarily contradict these previous reports. It is important to realize that the current technique is capable of detecting changes in metabolite levels much faster than previous NMR studies have achieved and thus variations in metabolite levels seen likely reflect earlier metabolic events.

In contrast to creatine phosphate levels, ATP levels are observed to change during the cycle. Comparison of panel A to panel C demonstrates that coincident to minimal P_i levels are maximal levels of β-ATP and vice versa. Because the resonance corresponding to β-ATP will necessarily change upon variation in ATP levels, this finding strongly suggests that net ATP hydrolysis occurs upon the onset of anoxia whereas net ATP synthesis occurs upon aerobic perfusion.

Results on α-ATP + NAD(H) levels (not shown) also vary by approximately 10–15% above and below mean values during the cycle. Careful examination of this resonance in difference spectra showed that much of the change could be accounted for by variation in NAD(H) levels. In fact, during the cycle NAD(H) levels varied from maximal to undetectable amounts (see spectra B and E in Figure 5). As mentioned above, this finding supports the previous report by Chance & Baltscheffsky (1958), who showed that variations in the mitochondrial energy state affect the binding of pyridine nucleotides

and thus likely its T_1 value.

Discussion

The effects of anoxia on ventricular function has been examined by many investigators in an effort to determine the primary event(s) responsible for contractile failure. Katz & Hecht (1969) have suggested that proton-induced disturbance in Ca^{2+} metabolism is primarily responsible for contractile failure. Under conditions of severe respiratory acidosis, increased $[H^+]$ does have a marked negative inotropic effect, independent of internal energy levels (Williamson et al., 1978). On the other hand, Hearse (1979) has concluded that, in the absence of severe acidosis, anoxia-induced depletion of internal energy stores causes contractile failure. In this study, Hearse (1979) showed that ATP and creatine phosphate levels declined by 25 and 50%, respectively, during the first 5 s of anoxia prior to a decline in contractile activity. More recently, Matthews et al. (1981a) have reexamined this problem using the ^{31}P NMR technique and concluded that neither acidosis nor a decline in cellular ATP levels is responsible for contractile failure and that more subtle mechanisms should be considered. These authors showed that, during the first 5 min of hypoxia, cardiac contractility declined dramatically prior to a decline in cellular ATP levels. They also showed that perfusion of hypoxic hearts with aerobic medium restored contractile function to prehypoxic levels without having fully reversed acidosis.

These discrepancies may be accountable, in part, due to differences in perfusion techniques used and methods used for metabolite analysis. Hearse (1979) examined the effects of anoxia on working hearts using the freeze–clamp technique whereas Matthews et al. (1981a) measured metabolite levels in Langendorff perfused hearts using the NMR method. As mentioned above the need for signal averaging largely prevents NMR measurements from resolving rapid metabolic events. The freeze–clamp technique approaches such resolution but is destructive and thus obscures any information concerning possible compartmentation of metabolites. In the present study, we have introduced the use of gating NMR measurements to an alternating aerobic–anoxic perfusion cycle to study the early effects of anoxia on cardiac energy metabolism. The clear advantage of this technique to previous studies is that very rapid events can now be measured, limited only by the time required to collect an FID.

The results obtained here show that intracellular pH and the levels of P_i, ATP, and NAD(H) vary during the perfusion cycle. Conspicuously absent from these spectra are elevated levels of sugar phosphates (see Figure 5) which have a chemical shift of 6.5–7.5 ppm relative to creatine phosphate (Ingwall, 1982). Sugar phosphate levels were elevated in hearts alternately perfused with medium containing glucose, but even these levels were low (results not shown). This finding, however, is consistent with the previous report by Williamson (1966), who showed that sugar phosphate levels do not increase until 10–15 s into anoxic perfusion.

The finding that the levels of ATP rather than creatine phosphate vary during the cycle is new, and we believe that it supports the hypothesis of a functional coupling between the adenine nucleotide translocase and mitochondrial bound creatine kinase (Bessman & Geiger, 1980; Saks et al., 1978; McClellen et al., 1983; Barbour et al., 1984). As a result of this coupling, matrix ATP transported across the inner membrane preferentially reacts with mitochondrial bound creatine kinase. By this mechanism inhibition of oxidative phosphorylation by anoxia should result in matrix ATP being preferentially utilized to maintain cytosolic creatine phosphate levels. This effect should only be a transient event, since mitochondrial matrix ATP levels, which account for approximately 15–20% of total cellular levels (Illingworth et al., 1975), would be rapidly consumed followed by a decline in creatine phosphate levels. The cytosolic breakdown of creatine phosphate to form ATP could thus act to maintain ATP levels until creatine phosphate levels are exhausted at which point ATP levels would then decline. Previous NMR studies that have measured changes in steady-state levels of metabolites on the time frame of minutes would thus be expected to detect only the latter phases of this sequence (i.e., a decline in creatine phosphate levels prior to a decline in ATP levels with the onset of anoxia).

In principle, the decline and recovery rates of metabolites shown to vary during the alternating perfusion cycle can be used to estimate minimal flux rates through these reactions. A minimal estimate for the net rate of ATP hydrolysis is determined by the observed rate of decline of its level during the cycle. On the other hand, minimal rates of ATP synthesis are equal to the sum of its decline and recovery rates. This is clear since ATP hydrolysis must be occurring at all times during the perfusion cycle. These values are considered minimal estimates since a small degree of oxidative phosphorylation will occur during anoxic perfusion due to the presence of low levels of oxygen in the medium (see Materials and Methods) and because the transition from aerobic to anoxic perfusion is not abrupt (see above). By use of a value of 25 μmol of ATP/g dry weight as the level of ATP in a well-oxygenated heart (Williamson, 1966), the approximate decline and recovery rates based on the line drawn through the data shown in Figure 6C are 4.0 and 2.6 μmol/s, respectively. This indicates that the net rates of ATP synthesis and hydrolysis are 396 and 240 μmol min^{-1} g^{-1} dry weight, respectively. That these initial rates differ is expected since a burst of ATP synthesis is required for overall levels to remain in steady state. Rates of ATP synthesis for working hearts perfused with pyruvate which exhibit similar hemodynamic activity (Kobayashi & Neeley, 1979) are 600 μmol/g^{-1} dry weight min^{-1} assuming a P/O ratio of 3. This value would thus represent a maximal rate of ATP synthesis. By this analysis, maximal and minimal rates of ATP turnover can be estimated. The above rate of ATP synthesis measured by alternating perfusion compares to a calculated rate of 840 μmol min^{-1} g^{-1} dry weight as determined by saturation transfer measurements which likely represents an overestimate due to the calculated P/O ratio of 3.5 (Matthews et al., 1981b).

The application of gating techniques to metabolic studies allows for the quantitative measurement of rapid metabolic processes. Recent examples of this technique are reports by Fossel et al. (1980) and Dawson et al. (1978, 1980), who examined the effects that the cardiac cycle and muscle fatigue have on high energy phosphate levels, respectively. The former group demonstrated that significant variations in the levels of ATP, creatine phosphate, P_i, sugar phosphates, and NAD(H) were detected during the cycle with total ATP and creatine phosphate levels changing by 35% within 107 ms between peak systole to diastole. In these studies the overall effect of muscle contraction on metabolism was examined. When alternating perfusion is combined with NMR gating, the present study has shown that the effects of individual metabolites (i.e., oxygen) on muscle metabolism can now be explored. We believe that this combination of techniques will likely have broad-based application to numerous systems studying not only phosphorus metabolism but, by using enriched isotopes, carbon and nitrogen metabolism as well.

Because this represents a new concept, we have defined below the conditions that we feel should be met to obtain meaningful information and discuss the limitations that the dynamics of coronary flow impose on the interpretation of results. Ideally, four requirements should be met when a metabolite gated-perfusion experiment is designed. These are the following: (a) the periodic application of an agent should result in a transient perturbation of metabolism from steady state, (b) the effect of the agent should be rapidly and uniformly distributed throughout the tissue, (c) the onset of this effect should be rapid relative to the duration of the perturbation, and (d) the system under study should remain physiologically stable to this perturbation during the time course of the experiment. In addition, if conditions b and c are to be met, then the rate of tissue perfusion must be rapid, and the tissue should have very high affinity for the agent, be able to consume it rapidly, and have little capacity to accumulate the agent.

The choice of oxygen for this type of measurement is ideally suited. It is well established that the heart has little capacity to store oxygen. Fabel (1968) has calculated that, on the basis of the myoglobin levels and the amount of physically dissolved oxygen, oxygen reserves in the heart are approximately 200 nmol g^{-1} dry weight. Kobayashi & Neeley (1979) have determined that working rat hearts can consume oxygen at a rate as high as 100 μmol g^{-1} dry weight min^{-1}. Comparing this value to that obtained by Fabel indicates that total oxygen reserves in the heart can be utilized within 110 ms upon the onset of anoxia. This value corresponds well with results recently reported by Chance and co-workers (Tamura et al., 1978), who showed that following an ECG pulse, approximately 10% of cellular myoglobin, undergoes an oxygenation–deoxygenation cycle and that measurable changes in steady-state O_2 tension could be detected in 3 ms.

The utilization of oxygen in the heart is dependent on the dynamics of coronary circulation and its intrinsic rate of consumption. Coronary flow rates and oxygen consumption vary during the cardiac cycle (Kirk & Honig, 1964) and with depth of the tissue (Klocke, 1976). Highest rates of oxygen consumption occur during peak systolic contraction in the endomyocardial layer (Weiss, 1973), whereas minimal flow rates exist under these conditions (Kirk & Honig, 1964).

In evaluating the effects of the O_2/N_2 perfusion cycle on myocardial metabolism it is important to consider the dynamic changes which occur upon the onset of anoxia. The dynamics of oxygen consumption in the heart are complex. Weiss (1973) has measured the mean steady-state tissue oxygen tension for a beating dog heart in situ using a micro oxygen electrode. He reported that oxygen tensions were greater in the epicardial than the endocardial layer (26 vs. 19 mmHg) and that, upon increased heart rate, endocardial oxygen tensions decreased disproportionally faster.

Chance (1971) has investigated the dynamics of oxygen consumption in the heart at the cellular level and has elegantly demonstrated that there likely exist very steep oxygen gradients within the tissue. Using NADH fluorescence photography, Steenbergen et al. (1978) have shown that tissue exposed to high flow hypoxia is not uniformly anoxic but rather consists of a stable heterogeneous distribution of anoxic zones. A gradual increase in perfusate oxygen levels also showed that the last area of tissue to become anoxic is the first to resume aerobic metabolism. These observations indicate that the development of anoxic zones is not a random event. When photographs of surface NADH were compared to thioflavin-S fluorescence, it was shown that anoxic zones consist of clusters of cells located in underperfused regions. This finding is surprising since it is known that hypoxia increases coronary flow. It appears, therefore, that, during severe hypoxia, local perfusion is not uniformly increased.

Reasons for such heterogeneity in oxygen consumption likely results from the known biochemical, morphological, and mechanical differences which exist in the various regions of the heart. Whitty et al. (1978) have demonstrated that mitochondria isolated from the subendocardial layer of canine myocardium are smaller in size, are more vulnerable to anoxic injury, and have greater efficiency for ATP synthesis than mitochondria isolated from the subepicardial layer. In addition, it is well established that in a beating heart transmural pressure gradients exist (Ellis & Klocke, 1979), and as a result, coronary perfusion varies during the cardiac cycle with respect to time and depth of tissue. During peak systolic contraction coronary flow in the endocardial layer is greatly reduced (Kirk & Honig, 1964; Klocke, 1976) whereas higher flow rates occur in the epicardial layer. Transmural gradients of coronary flow are also influenced by the preload conditions with lower flow rates occuring in diastole in the endocardial layer at higher preload pressures (Weiss, 1973). On the basis of the above discussion it seems clear that at any given moment the rate of oxygen consumption is heterogeneous, and therefore, upon the onset of anoxia there will be a similar heterogeneous deline in the levels of internal energy stores. NMR measurements made during such a decline (or recovery) will therefore measure the average rate of decline (or recovery) of these metabolites. It should be emphasized that this limitation does not detract from the utility of this technique since although the changes in metabolite levels observed represent an averaged value throughout the tissue, such changes are real and can be resolved on a very rapid time scale.

The success of an alternating perfusion NMR gating experiment depends upon measuring the same response to the perturbations at each data acquisition location in the cycle for the duration of the experiment. Any change in cardiac performance during the cycle will tend to "smear out" the effects of the perturbation and render differences less apparent in metabolite levels between data acquisition. A significant amount of the variability can be removed by pacing the heart during the experiment to ensure constant performance (Hollis et al., 1978; Fossel et al., 1980). In addition, minimizing the dead volume between the perfusate junction and the heart should also improve precision between hearts.

A difficulty encountered in these studies was to know precisely when the heart was maximally anoxic or aerobic. An estimate of this time is 4–4.5 s (see above) following the TTL pulse to open the nitrogen and oxygen lines, respectively. On the basis of the results shown in Figure 6, it appears that the biochemical response to alternating perfusion is out of phase from the gated-perfusion sequence by approximately 2 s. This may reflect the additional time required for complete perfusion of the coronary bed to occur and the time for oxygen to diffuse from the coronary to the mitochondrial membrane. For example, Franke et al. (1976) have estimated the latter parameter in perfused kidney and determined that the half-time for NADH oxidation is 125 ms.

One approach of locating the largest change in metabolite levels during the cycle, using a single heart, would be to spike the N_2 perfusate with a metabolically inert phosphorus-containing compound whose peak area in the spectrum would reflect the extent of N_2 perfusion at that point in the cycle. While conceptually straightforward, there is some difficulty generating a standard curve that relates the peak area and the

degree of N_2 perfusion. Essentially several points on the leading edge of the N_2 perfusate front must be sampled in order to plot the curve.

Alternately, future experiments on the measurement of the "steady-state" rate of ATP synthesis during O_2/N_2 perfusion cycle using the saturation transfer technique should be possible. Chemical exchange processes in vivo can be investigated by using NMR by the saturation transfer technique (Forsen & Hoffman, 1964; Campbell et al., 1978) if the rate constant is of the same order of magnitude as T_1. This technique has been employed in perfused hearts to measure the steady-state rate of ATP synthesis under different conditions (Matthews et al., 1981b; Nunnally & Hollis, 1979). Saturation transfer measurements have also been gated to the cardiac cycle to measure differences in rates of ATP synthesis between systole and diastole. It should be possible to apply this technique to measure differences in rates of ATP synthesis during this aerobic/anoxic cycle.

In conclusion, the current study introduces the technique of metabolite-perfused gating (specifically aerobic/anoxic cycle) in an NMR experiment to examine the effects that transient anoxia has on cellular energy metabolism in perfused hearts. This method should be applicable to a wide variety of systems to examine the effects that various agents (i.e., metabolites, drugs, hormones, etc.) have on various aspects of intermediary metabolism.

Acknowledgments

We thank Michael Tafler for his technical assistance in designing and fabricating the hardware interface.

Registry No. ATP, 56-65-5; NADH, 58-68-4; NAD, 53-84-9; O_2, 7782-44-7; phosphate, 14265-44-2; creatine phosphate, 67-07-2.

References

Ackerman, J. J. H., Gadian, D. G., Radda, G. K., & Wong, G. G. (1981) *J. Magn. Reson. 42*, 498–500.

Bailey, I. A., & Seymour, A. L. (1981) *Biochem. Soc. Trans. 9*, 234–236.

Bailey, I. A., Seymour, A. L., & Radda, G. K. (1981) *Biochim. Biophys. Acta 637*, 1–7.

Barbour, R. L., Sotak, C. H., Levy, G. C., & Chan, S. H. P. (1983) *Fed. Proc., Fed. Am. Soc. Exp. Biol. 42*, 2060 (Abstract 1770).

Barbour, R. L., Ribaudo, J., & Chan, S. H. P. (1984) *J. Biol. Chem. 259*, 8246–8251.

Bessman, S., & Geiger, P. (1981) *Science (Washington, D.C.) 211*, 448–452.

Campbell, I. D., Dobson, C. M., Radcliffe, R. G., & Williams, R. J. P. (1978) *J. Magn. Reson. 29*, 397–417.

Chance, B. (1971) *Circ. Res., Suppl I*, I-69.

Chance, B., & Baltscheffsky, H. (1958) *J. Biol. Chem. 233*, 736–739.

Dawson, J. M., Gadian, D. G., & Wilkie, D. R. (1978) *Nature (London) 274*, 861–866.

Dawson, J. M., Gadian, D. G., & Wilkie, D. R. (1980) *Philos. Trans. R. Soc. London, Ser. B B289*, 445–455.

Dumoulin, C. L., & Levy, G. C. (1981) *Comput. Chem. 5*, 9–18.

Ellis, A. K., & Klocke, F. J. (1979) *Circ. Res. 46*, 68–77.

Fabel, H. (1968) in *Oxygen Transport in Blood and Tissue* (Lubbers, D. W., et al., Eds.) p 159–171, Stuttgart, George Thieme.

Flaherty, J. T., Weisfeldt, M. L., Bulkley, B. H., Gardner, T. J., Gott, V. L., & Jacobus, W. E. (1982) *Circulation 65*, 561–570.

Forsen, S., & Hoffman, R. A. (1964) *J. Chem. Phys. 40*, 1189–1196.

Fossel, T., Morgan, H. E., & Ingwall, J. S. (1980) *Proc. Natl. Acad. Sci. U.S.A. 77*, 3654–3658.

Franke, H., Barlow, C. H., & Chance, B. (1976) *Am. J. Physiol. 231*, 1082–1089.

Gadian, D. G. (1982) *NMR and Its Applications to Living Systems*, Oxford University Press, Oxford.

Gadian, D. G., Radda, G. K., Brown, T. L. Chance, E. M., Dawson, M. J., & Wilkie, D. R. (1981) *Biochem. J. 194*, 215–228.

Hearse, D. (1979) *Am. J. Cardiol. 44*, 1115–1121.

Hollis, D. P., Nunnally, R. L., Taylor, G. J. N., Weisfeldt, M. L., & Jacobus, W. E. (1978) *J. Magn. Reson. 29*, 319–330.

Illingworth, J. A., Ford, W. C. L., Kobayashi, K., & Williamson, J. R. (1975) in *Recent Advances in Studies on Cardiac Structure and Metabolism* (Roy, P.-E., & Harris, P., Eds.) Vol. *8*, p 281, University Park Press, Baltimore, MD.

Ingwall, J. S. (1982) *Am. J. Physiol. 242*, H729–H744.

Jacobus, W. E. Pores, I. H., Lucas, S. K., Kallman, C. H., Weisfeldt, M. L., & Flaherty, J. T. (1982) in *Intracellular pH: Its Measurement, Regulation and Utilization in Cellular Functions*, pp 537–656, Alan R. Liss Publishing, New York.

Katz, A. M., & Hecht, H. H. (1969) *Am. J. Med. 47*, 497–502.

Kirk, E. S., & Honig, C. R. (1964) *Am. J. Physiol. 207*, 661–668.

Klocke, F. J. (1976) *Prog. Cardiovasc. Dis. 19*, 117–166.

Kobayashi, K., & Neely, J. R. (1979) *Circ. Res. 44*, 166–175.

Krebs, H. A., & Henseleit, K. (1932) *Hoppe-Seyler's Z. Physiol. Chem. 210*, 33–36.

Langendorff, O. (1895) *Pflugers Arch. Gesamte Physiol. Menschen Tiere 61*, 291–332.

Matthews, P. M., Radda, G. K., & Taylor, D. J. (1981a) *Biochem. Soc. Trans. 9*, 236–237.

Matthews, P. M., Bland, J. L., Gadian, D. G., & Radda, G. K. (1981b) *Biochem. Biophys. Res. Commun. 103*, 1052–1059.

McClellan, G., Weisberg, A., & Winegrad, S. (1983) *Am. J. Physiol. 245*, C423–427.

Morgan, H. E., Henderson, M. J., Regen, D. M., & Park, C. R. (1961) *J. Biol. Chem. 236*, 253–261.

Neeley, J. R., & Rovetto, M. J. (1975) *Methods Enzymol. 39*, 43–60.

Neeley, J. R., Liebermeister, H., Battersby, E. J., & Morgan, H. E. (1967) *Am. J. Physiol. 212*, 804–814.

Nunnally, R. L., & Hollis, D. P. (1979) *Biochemistry 18*, 3642–3646.

Saks, V. A., Rosenshtraukh, L. V., Smirnov, V. N., & Chazov, E. I. (1978) *Can. J. Physiol. Pharmacol. 56*, 691–706.

Steenbergen, C., Williamson, J. R., & DeLeew, G. J. (1978) in *Frontiers of Biological Energetics: Electrons to Tissues* (Dutton, P. L., Leight, J. S., & Scarpa, A. Eds.) Vol. II, pp 1541–1550, Academic Press, New York.

Tamura, M., Oshino, N., & Chance, B. (1978) *Recent Adv. Stud. Card. Struct. Metab. 11*, 307–312.

Weiss, H. R. (1973) *Adv. Exp. Med. Biol. 37A*, 553–559.
Whitty, A. J., Dimino, M. J., Elefont, E. A., Hughes, G. W., & Repeck, M. W. (1978) *Recent Adv. Stud. Card. Struct. Metab. 11*, 349–354.
Williamson, J. R. (1966) *J. Biol. Chem. 241*, 5026–5036.
Williamson, J. R., & Corkey, B. (1969) *Methods Enzymol. 13*, 434–513.
Williamson, J. R., Steenberger, C., Deleeuw, G., & Barlow, C. H. (1978) *Recent Adv. Stud. Card. Struct. Metab. 11*, 521–531.

Structural and Dynamical Details of Cholesterol–Lipid Interaction As Revealed by Deuterium NMR†

Erick J. Dufourc,‡ Edward J. Parish, Sarawanee Chitrakorn, and Ian C. P. Smith*

ABSTRACT: Deuterium nuclear magnetic resonance of specifically deuterated α- and β-cholesterol and 1-myristoyl-2-(deuteriomyristoyl)-*sn*-glycero-3-phosphocholine (molar ratio 3:7, respectively, dispersed in water) was used to differentiate between pure angular fluctuations (segmental order parameter, S_α) and average orientations (geometrical parameter, S_γ) of C–^{2}H bonds with respect to the normal to the bilayer. Hence, the orientation of cholesterol within the lipid bilayer was determined. In addition, the side chain of β-cholesterol has been found to be as ordered as the condensed ring structure. Such information allows a quantitation of the disordering–ordering effect of cholesterol in biological membranes: through the quasi temperature independence of its "wobbling", β-cholesterol allows motion of the lipid acyl chains below T_c (the transition temperature of the pure lipid) and inhibits them above T_c. Cholesterol thus acts as a *regulatory* agent by maintaining the bilayer membrane in a liquid-crystalline state where the motions are axially symmetric and the local order high. The α-isomer of cholesterol has a disordering–ordering action similar to that found for β-cholesterol. However, α-cholesterol is less efficient in this regulatory role than is the β-isomer, especially at high temperatures. Moreover, α-cholesterol is inclined with respect to the bilayer normal, at physiological temperatures. In the presence of either α- or β-cholesterol, the lipid local order parameter manifests a step in its temperature dependence about T_c, indicating that even in mixed systems the lipid retains a "memory" of its phase transition. A loss of axially symmetric shapes of the deuterium powder spectra was observed at low temperatures [5 °C for β-cholesterol–1,2-dimyristoyl-*sn*-glycero-3-phosphocholine (DMPC) and 15 °C for α-cholesterol–DMPC], indicative of restricted axial motion. For a given bilayer depth and at elevated temperatures, the degree of ordering of cholesterol is higher than that of DMPC; this demonstrates that in mixed systems, measurement of the properties of one component does not necessarily yield also the properties of the others. The latter should be considered in all types of probe experiments used in membrane systems.

Cholesterol is a major component of plasma membranes, where it is often equimolar in concentration with the phospholipids (Gomperts, 1977). It has amphipathic properties due to the presence of a hydroxyl group and a hydrophobic body (the steroid skeleton and the aliphatic tail attached at C-17). It is expected that cholesterol will orient itself within a lipid bilayer with its long axis normal to the membrane surface in order to maximize the hydrophilic and hydrophobic interactions (Figure 1).

Although the dynamics and conformational properties of cholesterol-containing membranes have been extensively investigated by a wide variety of techniques such as electron spin resonance (ESR)[1] (Schreier-Muccillo et al., 1973; Neal et al., 1976) or ^{2}H NMR (Stockton & Smith, 1976; Brown & Seelig, 1978; Oldfield et al., 1978; Taylor et al., 1981, 1982), there is considerable lack of detail at the molecular level. Most of the above studies concluded that cholesterol has a "condensing" effect on the lipid fatty acyl chains at temperatures above that of the gel to liquid-crystalline phase transition, T_c, and a disordering action below T_c. In some cases, it was reported that the gel to liquid-crystalline phase transition of the lipid was removed by addition of high amounts of cholesterol (Davis et al., 1979).

Several modes of action have been postulated. One of them uses the ordering–disordering properties to suggest that the sterol molecule controls the membrane "fluidity" (Madden et al., 1979) whereas another alternative invokes a direct cholesterol–protein or cholesterol–lipid interaction without modification of the so-called "viscosity" of the membranes (Dahl et al., 1981). The present study of cholesterol–lipid interactions at the *molecular level* provides more insight than the less direct or less accurate methods used previously to formulate the above models. It also provides a basis for the analysis of cholesterol–polyene antibiotic–lipid interactions (Dufourc & Smith, 1984).

^{2}H NMR is a reliable technique to obtain molecular information on the flexibility and dynamics of lipid molecules (Davis, 1983; Smith, 1984). Through the synthesis of specifically deuterated DMPC or α- and β-cholesterols (Figure

† From the Division of Biological Sciences, National Research Council of Canada, Ottawa, Canada K1A 0R6 (E.J.D. and I.C.P.S.), and the Department of Chemistry, Auburn University, Auburn, Alabama 36849 (E.J.P. and S.C.). *Received February 23, 1984.* N.R.C.C. Publication No. 23823.

‡ Present address: Centre de Recherches Paul Pascal, Domaine Universitaire, 33405 Talence Cedex, France.

[1] Abbreviations: ESR, electron spin resonance; ^{2}H NMR, deuterium nuclear magnetic resonance; DSC, differential scanning calorimetry; DMPC, 1,2-dimyristoyl-*sn*-glycero-3-phosphocholine; egg PC, egg phosphatidylcholine; THF, tetrahydrofuran; TLC, thin-layer chromatography.

0006-2960/84/0423-6062$01.50/0